Atmos. Chem. Phys. Discuss., 13, 311–343, 2013
www.atmos-chem-phys-discuss.net/13/311/2013/
doi:10.5194/acpd-13-311-2013

Atmospheric Chemistry and Physics Discussions

Why unprecedented ozone loss in the Arctic in 2011? Is it related to climatic change?

J.-P. Pommereau[1], F. Goutail[1], F. Lefèvre[1], A. Pazmino[1], C. Adams[6], V. Dorokhov[2], P. Eriksen[3], R. Kivi[4], K. Stebel[5], X. Zhao[6], and M. van Rozendael[7]

[1]LATMOS, CNRS-Université de Versailles St Quentin, UMR8190, Guyancourt, France
[2]Central Aerological Observatory, Dolgoprudny, Russia
[3]Danish Meteorological Institute, Copenhagen, Denmark
[4]Finnish Meteorological Institute, Sodankyla, Finland
[5]Norwegian Institute for Air Research, Kjeller, Norway
[6]Department of Physics, University of Toronto, Toronto, Ontario, Canada
[7]Belgian Institute for Space Aeronomy (IASB-BIRA), Brussels, Belgium

Received: 24 October 2012 – Accepted: 21 December 2012 – Published: 7 January 2013

Correspondence to: J.-P. Pommereau (pommereau@aerov.jussieu.fr)

Published by Copernicus Publications on behalf of the European Geosciences Union.

Abstract

An unprecedented ozone loss occurred in the Arctic in spring 2011. The details of the event are re-visited from the twice-daily total ozone and NO_2 columns measurements of the eight SAOZ/NDACC (Système d'Analyse par Observation Zénitale/Network for Detection of Atmospheric Composition Changes) stations in the Arctic. It is shown that the total ozone depletion in the polar vortex reached 38 % (approx. 170 DU) by the end of March that is larger than the 30 % of the previous record in 1996. Asides from the long extension of the cold stratospheric NAT PSC period, the amplitude of the event is shown to be resulting from a record daily total ozone loss rate of 0.7 % day^{-1} after mid-February, never seen before in the Arctic but similar to that observed in the Antarctic over the last 20 yr. This high loss rate is attributed to the absence of NO_x in the vortex until the final warming, in contrast to all previous winters where, as shown by the early increase of NO_2 diurnal increase, partial renoxification is occurring by import of NO_x or HNO_3 from the outside after minor warming episodes, leading to partial chlorine deactivation.

The cause of the absence of renoxification and thus of high loss rate, is attributed to a vortex strength similar to that of the Antarctic but never seen before in the Arctic. The total ozone reduction on 20 March was identical to that of the 2002 Antarctic winter, which ended around 20 September, and a 15-day extension of the cold period would have been enough to reach the mean yearly amplitude of the Antarctic ozone hole. However there is no sign of trend since 1994, neither in PSC volume, early winter denitrification, late vortex renoxification, and vortex strength nor in total ozone loss. The unprecedented large Arctic ozone loss in 2011 appears to resulting from an extreme meteorological event and there is no indication of possible strengthening related to climate change.

ACPD
13, 311–343, 2013

1 Introduction

An unprecedented stratospheric ozone loss has been reported in the Arctic by all ground-based, sondes and satellites observations during the winter 2010–11 (Manney et al., 2011; Sinnhuber et al., 2011, Arnone et al., 2012; Lindenmaier et al., 2012; Adams et al., 2012). It was mainly attributed to unusually long-lasting cold stratospheric conditions allowing Polar Stratospheric Clouds (PSCs) to form until late March. Chlorine activation and ozone loss was found comparable to that in the Antarctic ozone hole. But the warmer conditions, the lesser denitrification (removal of nitric acid) and the absence of dehydration, suggest that Arctic ozone holes are possible even with temperature much milder than those in the Antarctic (Manney et al., 2011, Arnone et al., 2012, Sinnhuber et al., 2011). Although an increase of PSC formation during the last three decades due to the cooling of the stratosphere has been suggested (Rex et al., 2004; WMO, 2011) and the eventuality of a large depletion in case of unusually cold winter has been recognised for long (WMO, 2011), such extreme loss was unpredicted by climate models. On the contrary, climate models are suggesting a progressive decrease of ozone depletion following the global reduction of concentration of Ozone Depleting Substances (ODS), faster in the Arctic than in the Antarctic because of the warmer stratosphere in the North (WMO, 2011). The question is thus to understand the reason for the unprecedented ozone loss in 2011, why it did not happen earlier and if it could happen again. For better understanding the details of the event, the time evolution of ozone loss and NO_2 during the winter was examined from the twice-daily measurements of the eight Arctic stations of the SAOZ/NDACC UV-Vis network. Section 2 describes the evolution of the loss during the winter and its relationship with stratospheric temperature, PSCs, denitrification and chlorine activation. The 2011 event is discussed by comparison to losses observed in the Arctic since 1994 in Sect. 3 and in the Antarctic in Sect. 4. The results are summarised in Sect. 5.

ACPD
13, 311–343, 2013

2 How much ozone loss in and out vortex in 2011

The ozone loss is determined by the "passive ozone" method, which consists to compare the total ozone columns measured by the SAOZ (Système d'Analyse par Observation Zénitale) UV-Vis spectrometer stations of the NDACC (Network for Detection of Atmospheric Composition Changes) to the "passive" ozone column predicted by a chemistry-transport model in the absence of chemistry (Goutail et al., 1999).

2.1 Tools

The data are those of eight SAOZ stations distributed around the Arctic (Table 1) providing measurements at Solar Zenith Angle up to 91°, that is throughout all the winter at the polar circle, but only after the return of the sun at higher latitude (Pommereau and Goutail, 1988). Total ozone is retrieved in the visible Chappuis bands (version V2, precision 4.5 %, total accuracy 5.9 %) with the spectral analysis and Air Mass Factor (AMF) settings recommended by the NDACC UV-Vis Working Group (Hendrick et al., 2011). The ozone columns used are sunrise-sunset means. NO_2 morning and evening columns are also available with 10–15 % accuracy.

The ozone loss is derived by comparison with the ozone columns of the REPROBUS Chemistry Transport Model (CTM) (Lefèvre et al., 1994) run in passive mode that is without chemistry. Winds and temperatures used to drive the CTM are those of the ECMWF ERA-Interim reanalyses (Simmons et al., 2006). REPROBUS was initialized on 1 December 2010 and was integrated on 60 vertical levels from the surface to 0.1 hPa, with a horizontal resolution of $2° \times 2°$. The comprehensive chemical package includes 45 chemical species and a "passive ozone" tracer. This tracer is initialized identically to ozone at the beginning of the simulation but is only transported by the winds without any chemical production or loss. This allows diagnosing the ozone chemical loss by making the difference between the "passive ozone" column calculated every day by the model over each station and the ozone column measured by SAOZ. In addition, the model provides for each station the ozone column calculated by a simulation

ACPD
13, 311–343, 2013

ignoring the heterogeneous processes. This "gas-phase" run is used to quantify the contribution of PSCs to the observed ozone loss.

The location of the station in reference to the vortex is provided by the potential vorticity (PV) on isentropic surfaces calculated by the MIMOSA contour advection model (Hauchecorne et al., 2002), where the vortex edge is defined as the maximum PV gradient (Nash et al., 1996).

2.2 Ozone loss over Sodankyla

As an example, Fig. 1 shows the analysis of the SAOZ ozone and NO_2 measurements in Sodankyla in Northern Finland from 1 December 2010 until 15 April 2011. During the darkest period until about 15 January, there is no difference (inside or outside of the vortex) between "passive", "gas phase", and SAOZ ozone columns. The NO_2 column is small with no diurnal variation but shows some sporadic spikes due to tropospheric pollution originating from Western Europe (Goutail et al., 1994). The further evolution is significantly different inside and outside of the vortex. Outside of the vortex, the difference between the SAOZ and the passive ozone columns builds-up after mid-January, reaching about 40 DU (10 %) at the end of March. Inside the vortex, the difference reaches 50 DU (12 %) around 10 February and 170 DU (40 %) in late March. The difference between SAOZ and the gas-phase simulation is 120 DU in late March. Asides from sporadic tropospheric pollution episodes (Goutail et al., 1994), NO_2 shows smaller columns inside than outside the vortex. Moreover NO_2 shows a diurnal increase of smaller amplitude inside the vortex, absent during the overpass of the vortex above the station around 10 February, and still limited by the end of March. Since the spring increase of NO_x concentration is originating from the photolysis of HNO_3, those features are indicative of a strong denitrification (HNO_3 removal by sedimentation of nitric acid rich NAT particles) in the vortex.

ACPD
13, 311–343, 2013

2.3 Mean ozone loss and denitrification/denoxification in and out vortex

The mean ozone loss is given by the 10-day average difference between SAOZ and passive ozone columns above the eight SAOZ stations as represented in Figs. 2 and 3 for respectively the inside and the outside of the vortex respectively. Also shown in the figures are the NO_2 sunrise and sunset columns above the same stations.

The ozone depletion diagnosed in the vortex shows two phases: an early loss that reaches 11 % on 10 February at an average rate of 0.2 % day^{-1}, followed by 40 days until 20 March of faster depletion at an average rate of 0.7 % day^{-1}. The first phase corresponds to the period of low solar illumination and inhomogeneous loss in the vortex when the depletion is restricted to a ring area at the inner edge (Goutail et al., 2005). The loss derived from each station is thus very dependent on its location relative to the centre of the vortex, resulting in a large dispersion between individual measurements. During the second phase, when the sun reaches SAOZ stations at higher latitude, the amount of data increases and the loss becomes more homogeneous. The total ozone loss in the vortex calculated at the end of the winter was 38 ± 5 % (approx. 170 DU), among which 12 % (50 DU) would be due to gas phase chemistry, mainly by HO_x-NO_x catalytic reactions, according to the REPROBUS model.

In contrast, outside the vortex (Fig. 3), the ozone chemical loss starts in early January at a mean rate of 0.2 % day^{-1}. The accumulated loss is showing a total ozone reduction of about 20 % (80 DU) by mid-April, entirely attributed to gas-phase chemistry by the model. This loss is larger than the gas-phase loss inside of the vortex because of the larger HO_x-NO_x concentration, the higher sun and the longer day. There is no indication there of a significant contribution from activated halogens.

The NO_2 columns shown in Figs. 2 and 3 are restricted to polar circle latitude stations to avoid the latitude dependent duration of the day and noontime SZA. Asides from the noise due to pollution episodes particularly in Sodankyla and Salekhard, the picture is significantly different in the inside and the outside of the vortex. In the inside (bottom panel of Fig. 2) the NO_2 column is low until mid-March, followed by a rapid

ACPD
13, 311–343, 2013

growth of both total amounts and diurnal cycle amplitude. In contrast, outside the vortex (bottom panel of Fig. 3) the NO_2 columns and the amplitude of the diurnal variation increase sooner, in early February. The best indicator of this difference, less sensitive to tropospheric pollution episodes, is the amplitude of the NO_2 diurnal cycle shown in Fig. 4. The late increase of its amplitude inside the vortex compared to earlier increase in the outside, is an indication of the absence of NO_x species implying a large removal of HNO_3 and a delayed formation of $ClONO_2$ and thus chlorine deactivation inside the vortex as reported by MLS/AURA (Manney et al., 2011), MIPAS/ENVISAT (Arnone et al., 2012) and the ground-based FTIR in Eureka (Lindenmaier et al., 2012).

2.4 Relation with temperature, denitrification and chlorine activation

Displayed in Fig. 5 are the minimum ERA-Interim temperatures poleward of 60° N at 475, 550 and 675 K, with the NAT threshold temperature formation (T_{NAT}) at the same levels. T_{NAT} is calculated from the formula of Hanson and Mauersberger (1988) and the MIPAS water vapour and nitric acid measurements in March 2011 (Arnone et al., 2012). As shown in Table 2, T_{NAT} was colder in March 2011 than the previous winters average by 1 K at 475 and 550 K because of the 2 ppb lower HNO_3 concentration. NAT PSCs were thermodynamically possible from mid-December onwards at all levels, extending until early March at 675 K, mid-March at 550 K and late March at 475 K. Remarkable are the extremely low temperatures at higher levels (181 K at 550 K, 178 K at 675 K) in early January where high altitude PSCs were observed by MIPAS (Arnone et al., 2012) followed by several periods of temperature below T_{NAT} at 475 and 550 K separated by minor warming episodes in mid January and early February resulting in deep denitrification as reported by MIPAS and MLS (Arnone et al., 2012, Manney et al., 2011).

Also displayed in Fig. 5 are: (i) the volume of NAT PSCs (V_{PSC}) between 400 and 675 K (13.5–23.5 km), (ii) the volume of sunlit NAT PSCs (sunlit V_{PSC}) weighted by the ratio between sunlit (SZA < 93°) and total vortex surface as an indicator of chlorine activated volume, and (iii) the integrated weighted sunlit V_{PSC} since the beginning of

ACPD
13, 311–343, 2013

the winter. According to ERA-Interim temperatures, PSCs have formed first in late December and early January at high altitude up to 675 K but of limited consequences for chlorine activation since mostly confined in the darkness. Later on they were present during the whole winter but at 475 and 550 K only after early February and at 475 K only after mid-March, but almost absent during four minor warming episodes in mid-January, early February and late March. Among all these most sunlit PSCs, those most favourable for chlorine activation, occurred between mid-February-mid-March. The question is which type of PSC is responsible for chorine activation and ozone loss. Figure 6 compares the ozone loss of Fig. 2 to the integrated sunlit V_{PSC} assuming that activation occurs at $T_{NAT} - 3$ K, T_{NAT} and $T_{NAT} + 3$ K, respectively. Although V_{PSC} increases from 0.1 to 0.6 and 1.45×10^9 km^3 at increasing threshold temperature, for better understanding the relationship between the time-evolution of PSC and ozone loss, V_{PSC} has been normalised at the date of the end of the ozone destruction on 30 March. V_{PSC} at $T_{NAT} - 3$ K corresponding to Supercooled Ternary Solution (STS) (Stein et al., 1999) is reducing rapidly after mid-February resulting in an end of O_3 loss 15 days earlier than observed. At the opposite, $T_{NAT} + 3$ K would delay it by 10 days. Best match is with PSC forming at T_{NAT}. Unless the ERA-Interim temperatures are biased, the observed ozone loss is fully consistent with chlorine remaining activated until NAT particles formation stops (i.e. at temperature warmer than 194 K at 50 hPa, approx. 19 km or 475 K).

3 Comparison with previous winters

The SAOZ/NDACC Arctic network has been providing daily ozone and NO_2 measurements since 1994 from which the relationship between ozone loss, denoxification and PSC volume calculated from the ERA Interim temperatures can be investigated.

ACPD
13, 311–343, 2013

3.1 Ozone loss

Figure 7 shows the total ozone loss derived from the SAOZ Arctic stations since 1994. For the sake of homogeneity, this analysis uses the ECMWF ERA-Interim reanalyses for all years instead of the operational analyses used in previous publications (WMO 2007). Significant changes are observed in the difference of temperature in the vortex between ERA-Interim and operational analysis. Indeed, operational analyses moved in late 1997 from a 31 levels 3-D variational assimilation to a 50 levels 4-D variational scheme including assimilation of the AMSU data, followed by a further change to 60 levels in late 1999. When compared to the temperatures measured in the vortex by long duration balloon between 30–146 hPa, operational temperatures showed insignificant bias of $+0.33 \pm 1.37$ K in 1997, dropping to -0.49 ± 0.91 K in 2000 (Pommereau et al., 2002; Knudsen et al., 2002). The difference between ERA Interim and operational analysis summarized in Table 3 suggests that operational analyses might be cold biased by 1–3 K depending on the year and altitude level.

The largest losses occurred in 1996 (30 %), 1997 (25 %), 2000 (23 %), 2003 (20 %), 2005 (23 %), 2008 (23 %) and 2011 (38 %). There is no trend since 1994 but high interanual variability in the depletion. Remarkably, the loss is never zero, even during years when little PSCs formed or when the vortex ended in January like in 1999, 2002 and 2004. The minimum 5 % depletion observed even in those years is consistent with an ozone reduction mainly caused by gas phase chemistry.

3.2 Ozone loss rate and denoxification

Figure 8, shows the detail of the evolution of temperature, ozone loss and NO_2 diurnal increase for the five years of largest ozone depletion. Among the five, 1997 was that of the longest stratospheric winter, ending around 30 March, and 1996 that of the largest depletion after 2011. But the most remarkable difference between 2011 and all other years is the fastest ozone loss rate of 0.7 % day^{-1} after 10 February compared to a maximum 0.35 %–0.45 % day^{-1} on all other years even during the sunlit March.

ACPD
13, 311–343, 2013

Another unique characteristic of 2011, consistent with this fast depletion rate, is the late increase of the NO_2 diurnal cycle that is the absence of NO_x and thus of chlorine deactivation until the final warming. This is in contrast with all previous years when the NO_x concentration started increasing well before the final warming. In 1996, the onset of the diurnal cycle of NO_2 occurred around 20 February, i.e. 20 days before the end of the ozone depletion period. In 1997, the year of the longest winter, it started around 20 January and amplified rapidly after 1 March, that is one month before the final warming. This fast increase of NO_2 was confirmed by measurements from long duration balloons navigating in the vortex (Denis et al., 2000). After 2011, the year of latest NO_2 diurnal increase is 2000. A major difference between 2011 and previous winters, is thus the amount of NO_x available, the rate-limiting step of chlorine deactivation by formation of $ClONO_2$ (Harris et al., 2010), confirmed by the late growth of $ClONO_2$ concentration at the 450 K reported by MIPAS after 20 March only in 2011 (Arnone et al., 2012). These late denitrification and chlorine deactivation are confirmed by the unusually low HNO_3 concentration and the large ClO amount at 485 K seen by MLS until late-March, similar to that observed in the Antarctic in September (Manney et al., 2011). Apart from the long duration of the cold stratospheric winter, the explanation for the record ozone depletion in the Arctic in 2011 is thus the fast loss rate after 10 February until the final warming because of the unprecedented late renoxification and chlorine deactivation.

Figure 9 shows the amplitude of the NO_2 diurnal cycle on each year on 1 February, 15 February, 1 March and 15 March since 1994. Early winter denitrification (removal of HNO_3) or at least denoxification (conversion of NO_x into HNO_3) after the formation of high altitude PSC (Rex et al., 2006; Harris et al., 2010; Pitts et al., 2011; Khosrawi et al., 2011; Arnone et al., 2012 and references herein), is common such as in 1996, 2000, 2005, 2008, 2010 and 2011. Less frequent is the extension of at least partial denoxification of the vortex until early March such as in 1996, 1997 and 2000, the year of largest signal after 2011, the last being the one of longer persistence of denoxification. The explanation is in the unusual strength of the vortex in 2011 shown by the maximum PV gradient larger than on all previous years (Fig. 10) as pointed out by

ACPD
13, 311–343, 2013

Manney et al. (2011), which prevented renoxification by mixing with NO_x- and HNO_3 gas phase rich air masses from the outside of the vortex as frequently observed in the Arctic after minor warming episodes and subsequent elongation and reformation of the vortex. However, as for the ozone loss in Fig. 7 or denoxification in Fig. 9, there is no sign of trend in the vortex strength since 1994, but only high inter-annual variability.

3.3 Relation between O_3 loss and PSC volume

The integrated PSC volume indicative of PSC vertical extension and duration has been proposed as proxy of total ozone loss each year (Rex et al., 2004, 2006; Harris et al., 2010). Displayed in Fig. 11 is the yearly sunlit V_{PSC} between 400–675 K since 1994 derived from ERA-Interim temperatures. The sunlit PSC volume was not larger in 2011 than in 1996. In that case also there is not sign of trend but of high variability. Figure 12 shows the relationship between SAOZ losses and integrated V_{PSC} between 400–675 K for the whole vortex on the left and sunlit only on the right. The non-zero intercept is consistent with a pure gas-phase ozone loss in the absence of PSC like in 1999 and 2002. Although the ozone loss shows better correlation with sunlit V_{PSC} (0.95) than with total V_{PSC} (0.88), this proxy only cannot explain the larger ozone loss in 2011. Another parameter is required, the state of denoxification controlling chlorine deactivation.

4 Comparison with the Antarctic

The yearly total ozone loss in the Arctic is compared in Fig. 13 to that of the Antarctic calculated with the same passive ozone method from ground-based and satellite data (adapted from Kuttippurath et al., 2010). Figure 13 suggests that for the pre-1992 period the amplitude of the Antarctic ozone hole was comparable to the Arctic in 2011. The amplitude of the 2011 Arctic depletion is of the same order of magnitude to that of the early warming winter of 2002 in the Antarctic when the depletion stopped during the second half of September (Stolarski et al., 2005), the equivalent of the second half

ACPD
13, 311–343, 2013

of March in the North, implying a loss process identical in the Arctic in 2011 to that observed every year in the Antarctic. This is confirmed by the similarity of the loss rate of 0.7 % day^{-1} derived by Kuttippurath et al. (2010) in the deeply denitrified Antarctic ozone hole after the formation of high altitude PSCs in the early winter in June and July (Pitts et al., 2007). The full denoxification is a typical feature of the SAOZ NO_2 columns measurements in the deeply denitrified Antarctic vortex where a diurnal variation was never observed in the vortex before the final warming.

The similarity of the ozone loss rate in the Arctic in 2011 with that occurring in the Antarctic over the last 20 yr indicates that for the first time, the process responsible was identical. A 15-day extension of the cold period until early April in the Arctic in 2011 would have been enough to reach an ozone hole amplitude similar to that of the Antarctic.

5 Conclusions

The reason for the unprecedented ozone loss in the Arctic in 2011 has been explored from the total ozone and NO_2 measurements of the eight SAOZ/NDACC UV-Vis stations deployed in the Arctic. The ozone depletion in the polar vortex reached 38 % (approx. 170 DU) in late March that is larger than the 30 % of the previous Arctic record in 1996. The cause of this 2011 record is shown to originate in the presence of NAT PSCs until late March in an unusually NO_x depleted vortex, resulting in a total ozone loss rate of 0.7 % day^{-1} never seen before in the Arctic but similar to that observed every year over the Antarctic. The cause of both the duration of the winter and the high loss rate is attributed to an unprecedented strength of the vortex, which prevented partial chlorine deactivation by NO_x or HNO_3 import from the outside as observed every year in the Arctic in contrast to the Antarctic where the vortex remains isolated during the full winter. The total ozone reduction at the end of the PSC period on 20 March was identical to that of the 2002 Antarctic winter, which ended around 20 September. There are no signs of trend since 1994, neither in PSC volume, amplitude of denitrification in

ACPD
13, 311–343, 2013

the early winter, renoxification of the vortex nor in total ozone depletion, which could suggest a relation with climate change. The unprecedented large Arctic ozone loss in 2011 appears to result from an extreme meteorological event only. From the SAOZ observations carried out since 1994 there is no information suggesting that the Arctic ozone loss could amplify or reduce in the future.

Acknowledgements. The authors are indebted to the personnel operating the SAOZ/NDACC stations and the ETHER data centre http://ether.ipsl.jussieu.fr/ for providing ECMWF analyses and reanalyses. The SAOZ measurements at Eureka were made with the support of the Canadian Network for the Detection of Atmospheric Change (CANDAC), led by James R. Drummond, and as part of the Canadian Arctic ACE Validation Campaigns, co-led by Kaley A. Walker and Kimberly Strong and funded by the Canadian Space Agency, Environment Canada, the Natural Sciences and Engineering Research Council, and the Northern Scientific Training Program. The SAOZ data are available at http://www.ndsc.ncep.noaa.gov/. The research was supported by the NDACC French programme funded by the CNRS Institut National des Sciences de l'Univers (INSU), the Centre National d'Etudes Spatiales (CNES) and the polar Institute Paul Emile Victor (IPEV), which are gratefully acknowledged.

The publication of this article is financed by CNRS-INSU.

References

Adams, C., Strong, K., Zhao, X., Bassford, M. R., Chipperfield, M. P., Daffer, W. H., Drummond, J. R., Farahani, E., Feng, W., Fraser, A., Goutail, F., Manney, G. L., McLinden, Pazmino, A. Rex, M., and Walker, K. A.: Severe 2011 ozone depletion assessed with

ACPD
13, 311–343, 2013

11 years of ozone, NO_2, and OClO measurements at 80° N, Geophys. Res. Lett., 39, L05806, doi:10.1029/2011GL050478, 2012.
Arnone, E., Castelli, E., Papandrea, E., Carlotti, M., and Dinelli, B. M.: Extreme ozone depletion in the 2010–2011 Arctic winter stratosphere as observed by MIPAS/ENVISAT using a 2-D tomographic approach, Atmos. Chem. Phys., 12, 9149–9165, doi:10.5194/acp-12-9149-2012, 2012.
Denis, L., Pommereau, J.-P., Lefèvre, F., Goutail, F., Knudsen, B., and Letrenne, G.: Ozone loss and NO_2 recovery during the winter and spring 1997 as observed from long duration balloons flights in the vortex, in: Proc. 5th European Ozone Workshop, European Commission Air Pollution Report 73, 4425–428, 2000.
Goutail, F., Pommereau, J.-P., Sarkissian, A., Kyro, E., and Dorohkov, V.: Total nitrogen dioxide at the Arctic polar circle since 1990, Geophys. Res. Lett., 21, 1371–1374, 1994.
Goutail, F., Pommereau, J.-P., Phillips, C., Deniel, C., Sarkissian, A., Lefèvre, F., Kyro, E., Rummukainen, M., Eriksen, P., Andersen, S. B., Kaastadt Hoiskar, B.-A., Braathen, G., Dorohkov, V., and Khattatov, V. U.: Total ozone depletion in the Arctic during the winters of 1993–1994 and 1994–1995, J. Atmos. Chem., 32, 1–34, 1999.
Goutail, F., Pommereau, J.-P., Lefèvre, F., van Roozendael, M., Andersen, S. B., Kåstad Høiskar, B.-A., Dorokhov, V., Kyrö, E., Chipperfield, M. P., and Feng, W.: Early unusual ozone loss during the Arctic winter 2002/2003 compared to other winters, Atmos. Chem. Phys., 5, 665–677, doi:10.5194/acp-5-665-2005, 2005.
Hanson, D. and Mauersberger, K.: Laboratory studies of the nitric acid trihydrate: implication for the south polar stratosphere, Geophys. Res. Lett., 15, 855–858, 1988.
Harris, N. R. P., Lehmann, R., Rex, M., and von der Gathen, P.: A closer look at Arctic ozone loss and polar stratospheric clouds, Atmos. Chem. Phys., 10, 8499–8510, doi:10.5194/acp-10-8499-2010, 2010.
Hauchecorne, A., Godin, S., Marchand, M., Heese, B., and Souprayen, C.: Quantification of the transport of chemical constituents from the polar vortex to midlatitudes in the lower stratosphere using the high-resolution advection model MIMOSA and effective diffusivity, J. Geophys. Res., 107, 8289, doi:10.1029/2001JD000491, 2002.
Hendrick, F., Pommereau, J.-P., Goutail, F., Evans, R. D., Ionov, D., Pazmino, A., Kyrö, E., Held, G., Eriksen, P., Dorokhov, V., Gil, M., and Van Roozendael, M.: NDACC/SAOZ UV-visible total ozone measurements: improved retrieval and comparison with correl-

ACPD
13, 311–343, 2013

ative ground-based and satellite observations, Atmos. Chem. Phys., 11, 5975–5995, doi:10.5194/acp-11-5975-2011, 2011.
Khosrawi, F., Urban, J., Pitts, M. C., Voelger, P., Achtert, P., Kaphlanov, M., Santee, M. L., Manney, G. L., Murtagh, D., and Fricke, K.-H.: Denitrification and polar stratospheric cloud formation during the Arctic winter 2009/2010, Atmos. Chem. Phys., 11, 8471–8487, doi:10.5194/acp-11-8471-2011, 2011.
Knudsen, B. M., Pommereau, J.-P., Garnier, A., Nunes Pinharanda, M., Denis, L., Newman, P. A., Letrenne, G., and Durand, M.: Accuracy of analysed stratospheric temperatures in the winter Aarctic vortex from infrared Montgolfier long-duration balloon flights. 2. Results, J. Geophys. Res., 107, 4316, doi:10.1029/2001JD001329, 2002.
Kuttippurath, J., Goutail, F., Pommereau, J.-P., Lefèvre, F., Roscoe, H. K., Pazmiño, A., Feng, W., Chipperfield, M. P., and Godin-Beekmann, S.: Estimation of Antarctic ozone loss from ground-based total column measurements, Atmos. Chem. Phys., 10, 6569–6581, doi:10.5194/acp-10-6569-2010, 2010.
Lefèvre, F., Brasseur, G. P., Folkins, I., Smith, A. K., and Simon, P.: Chemistry of the 1991–92 stratospheric winter: three dimensional model simulations, J. Geophys. Res., 99, 8183–8195, 1994.
Lindenmaier, R., Strong, K., Batchelor, R. L., Chipperfield, M. P., Daffer, W. H., Drummond, J. R., Duck, T. J., Fast, H., Feng, W., Fogal, P. F., Kolonjari, F., Manney, G. L., Manson, A., Meek, C., Mittermeier, R. L., Nott, G. J., Perro, C., and Walker, K. A.: Unusually low ozone, HCl, and HNO_3 column measurements at Eureka, Canada during winter/spring 2011, Atmos. Chem. Phys., 12, 3821–3835, doi:10.5194/acp-12-3821-2012, 2012.
Manney, G., Santee, M. L., Rex, M., Livesey, N. J., Pitts, M. C., Veefkind, P., Nash, R. R., Wohltmann, I., Lehmann, R., Froidevaux, L., Poole, L. R., Schoeberl, M. R., Haffner, D. P., Davies, J., Dorokhov, V., Gernandt, H., Johnson, B., Kivi, R., Kyr o, E., Larsen, N., Levelt, P. F., Makshtas, A., McElroy, C. T., Nakajima, H., Parrondo, M. C., Tarasick, D. W., von der Gathen, P., Walker, P. K. A., and Zinoviev, N. S.: Unprecedented Arctic ozone loss in 2011, Nature, 478, 469–475, doi:10.1038/nature10556, 2011.
Nash, E. R., Newman, P. A., Rosenfield, J. E., and Schoeberl, M. R.: An objective determination of the polar vortex using Ertel's potential vorticity, J. Geophys. Res., 101, 9471–9478, 1996.
Pitts, M. C., Thomason, L. W., Poole, L. R., and Winker, D. M.: Characterization of Polar Stratospheric Clouds with spaceborne lidar: CALIPSO and the 2006 Antarctic season, Atmos. Chem. Phys., 7, 5207–5228, doi:10.5194/acp-7-5207-2007, 2007.

ACPD
13, 311–343, 2013

Pitts, M. C., Poole, L. R., Dörnbrack, A., and Thomason, L. W.: The 2009–2010 Arctic polar stratospheric cloud season: a CALIPSO perspective, Atmos. Chem. Phys., 11, 2161–2177, doi:10.5194/acp-11-2161-2011, 2011.

Pommereau, J.-P. and Goutail, F.: O_3 and NO_2 ground-based measurements by visible spectrometry during Arctic winter and spring 1988, Geophys. Res. Lett., 15, 891–894, 1988.

Pommereau, J.-P., Garnier, A., Knudsen, B. M., Letrenne, G., Durand, M., Csersnjes, P., Nunes-Pinharanda, M., Denis, L., Vial, F., Hertzog, A., and Cairo, F.: Accuracy of analysed stratospheric temperatures in the winter Arctic vortex from infra red Montgolfier long duration balloon flights. Part I: Measurements, J. Geophys. Res., 107, 8260, doi:10.1029/2001JD001379, 2002.

Rex, M., Salawitch, R. J., von der Gathen, P., Harris, N. R. P., Chipperfield, M. P., and Naujokat, B.: Arctic ozone loss and climate change, Geophys. Res. Lett., 31, L04116, doi:10.1029/2003GL018844, 2004.

Rex, M., Salawitch, R. J., Deckelmann, H., von der Gathen, P., Harris, N. R. P., Chipperfield, M. P., Naujokat, B., Reimer, E., Allaart, M., Andersen, S. B., Bevilacqua, R., Braathen, G. O., Claude, H., Davies, J., De Backer, H., Dier, H., Dorokov, V., Fast, H., Gerding, M., Godin-Beekmann, S., Hoppel, K., Johnson, B., Kyro, E., Litynska, Z., Moore, D., Nakane, H., Parrondo, M. C., Risley, A. D., Skrivankova, P., Stubi, R., Viatte, P., Yushkov, V., and Zerefos, C.: Arctic winter 2005: implications for stratospheric ozone loss and climate change, Geophys. Res. Lett., 33, L23808, doi:10.1029/2006GL026731, 2006.

Simmons, A. J., Uppala, S. M., Dee, D., and Kobayashi, S.: ERAInterim: new ECMWF reanalysis products from 1989 onwards, ECMWF News Lett., 110, 25–35, 2006.

Sinnhuber, B.-M., Stiller, G., Ruhnke, R., von Clarmann, T., Kellmann, S., and Aschmann, J.: Arctic winter 2010/2011 at the brink of an ozone hole, Geophys. Res. Lett., 38, L24814, doi:10.1029/2011GL049784, 2011.

Stein, B., Wekind, C., Wille, H., Immler, F., Mullere, M., Woste, L., del Guasta, M., Morandi, M., Stefanutti, L., A,tonell, A., Agostini, P., Rizi, V., Readelli, G., Mitev, V., Matthey, R., Kivi, R., and Kyro, E;: Optical classification, existence temperatures, and coexistence of different stratospheric cloud types, J. Geophys. Res., 1042, 23983–23994, doi:10.1029/1999JD900064, 1999.

Stolarski, R. S., McPeters, R. D., and Newman, P. A.: The ozone hole of 2002 as measured by TOMS, J. Atmos. Sci., 62, 716–720, 2005.

ACPD
13, 311–343, 2013

WMO (World Meteorological Organization): Scientific assessment of ozone depletion: 2006, Global Ozone Research and Monitoring Project–Report 50, Geneva, Switzerland, 2007.
WMO (World Meteorological Organisation): Scientific assessment of ozone depletion: 2010, Global Ozone Research and Monitoring Project, Report 52, Geneva, Switzerland, 516 pp., 2011.

ACPD
13, 311–343, 2013

Table 1. SAOZ Arctic stations.

Eureka, Nunavut	80° N, 86° W
Ny-Alesund, Svalbard	78° N, 12° E
Thule, Greenland	76° N, 69° W
Scoresbysund, Greenland	71° N, 22° W
Sodankyla, Finland	67° N, 27° E
Salekhard, Russia	67° N, 67° E
Zhigansk, Russia	67° N, 123° E
Harestua, Norway	60° N, 11° E

ACPD
13, 311–343, 2013

Table 2. Threshold temperature of NAT and ICE formation calculated for March 2011 and Arctic mean, from monthly average HNO_3 and H_2O concentrations reported by MIPAS (Arnone et al., 2012).

Theta (K)	Alt. (km)	H_2O (ppm)	HNO_3 2011 (ppb)	T_{NAT} 2011 (K)	HNO_3 Mean (ppb)	T_{NAT} Mean (K)	T_{ICE} (K)
475	20.2	4.6	6	194	8	195	187
550	23.7	5.0	6	191	8	192	185
675	28.5	5.5	5	187	5	187	182

ACPD
13, 311–343, 2013

Table 3. ERA Interim – ECMWF operational analyses mean difference of minimum temperature poleward of 60° N in the winter between 1994 and 2012.

Year	ΔT 475 K	ΔT 550 K
1994	0	0
1995	0	0
1996	0	0
1997	0	0
1998	0	2.6
1999	0	3.6
2000	1.0	2.0
2001	0	3.4
2002	0.8	2.6
2003	1.6	3.0
2004	1.7	1.0
2005	1.9	1.7
2006	2.4	1.7
2007	1.3	2.1
2008	2.1	2.6
2009	1.6	1.8
2010	2.3	2.3
2011	2.4	1.8
2012	0.5	0.9

ACPD
13, 311–343, 2013

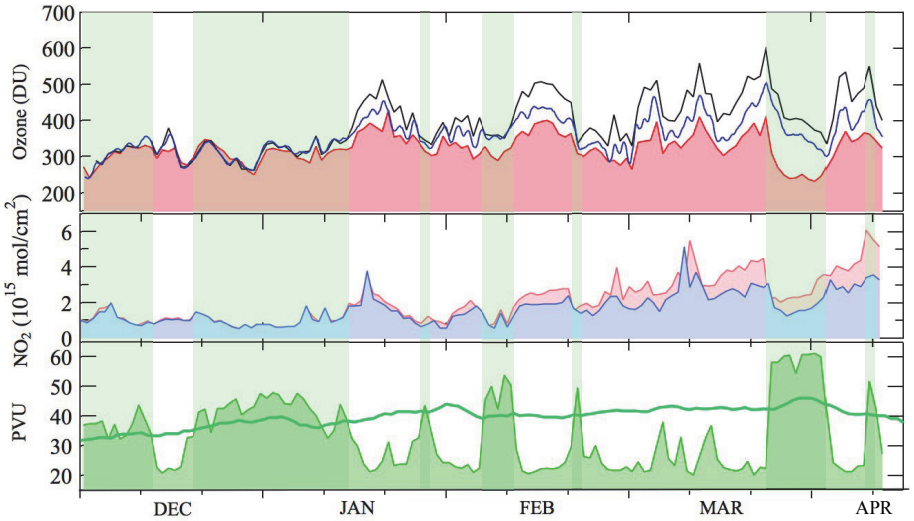

Fig. 1. SAOZ measurements in Sodankyla from 1 December 2010 to 15 April 2011. From top to bottom: SAOZ total ozone (pink filled area) compared to REPROBUS passive ozone (black line) and gas-phase chemistry only (blue line); SAOZ NO_2 column (sunrise blue, sunset red); and potential vorticity at 475 K (green filled area) and limit of the vortex (thick line). Light green shaded areas are showing the periods when the vortex was present above the station.

ACPD
13, 311–343, 2013

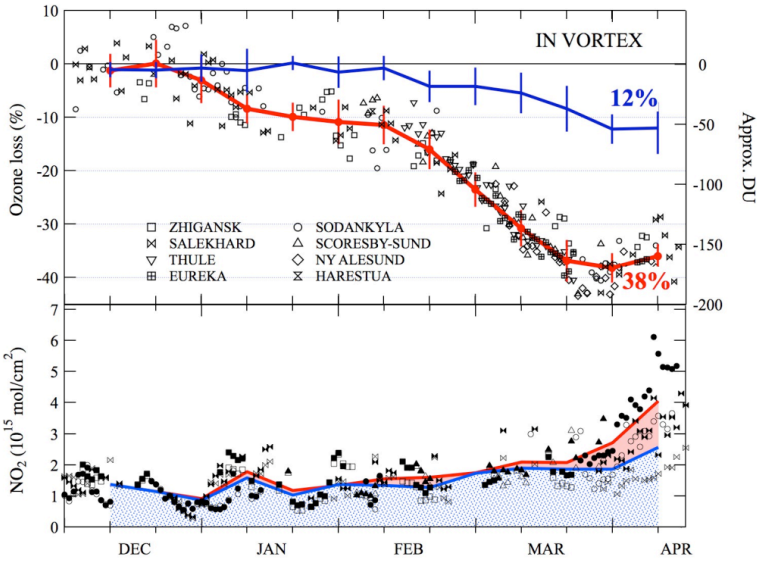

Fig. 2. Ozone loss (top) and total NO_2 (bottom) in the vortex. The ozone loss is given by the difference between SAOZ and passive ozone columns where markers are representing the loss above each station and the red line 10-day averages with dispersion. The blue line is the difference between passive ozone and gas phase REPROBUS simulations. A 12 % total loss at an average rate of 0.2 % day^{-1} is observed between 20 December and 10 February, followed by a faster depletion at 0.7 % day^{-1} until 20 March. The total loss at the end of the winter compared to a pure ozone tracer is reaching 38 ± 5 % and 26 % compared to the gas phase simulation. The evolution of the NO_2 column in the bottom panel (open markers and blue line at sunrise, filled markers and red line at sunset) is showing low values until mid-March, increasing rapidly after. The amplitude of the NO_2 diurnal cycle remains limited until 20 March and enhances rapidly after.

ACPD
13, 311–343, 2013

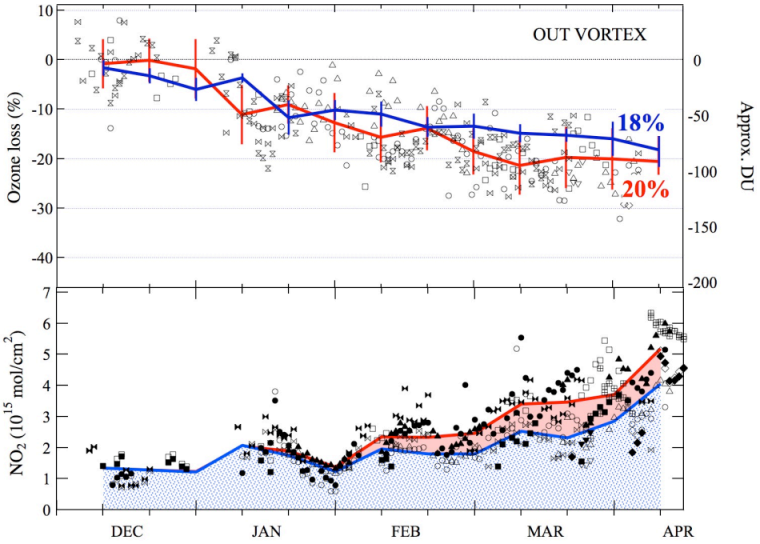

Fig. 3. Same as Fig. 2 but outside the vortex. The ozone depletion derived from the difference between SAOZ and passive ozone is very similar to that simulated by the model in gas phase chemistry only. There is no indication of significant contribution from heterogeneous chlorine activation. The NO_2 column and its diurnal variation begin to increase in early February, one and half month sooner than in the inside.

ACPD
13, 311–343, 2013

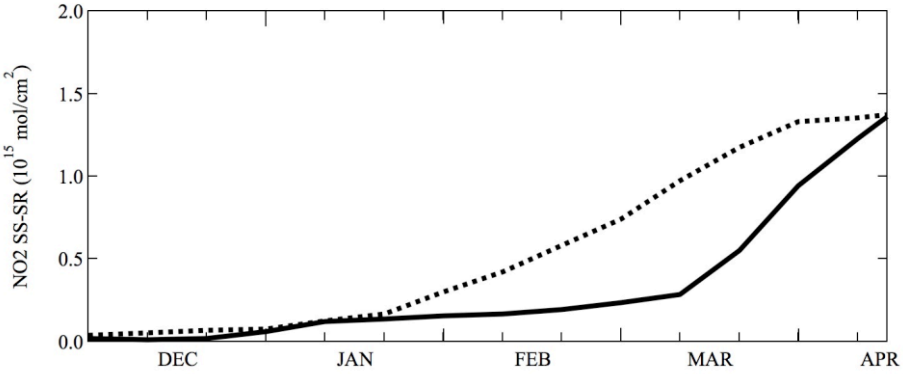

Fig. 4. Amplitude of the NO_2 diurnal cycle inside (solid line) and outside (dotted line) the vortex.

ACPD
13, 311–343, 2013

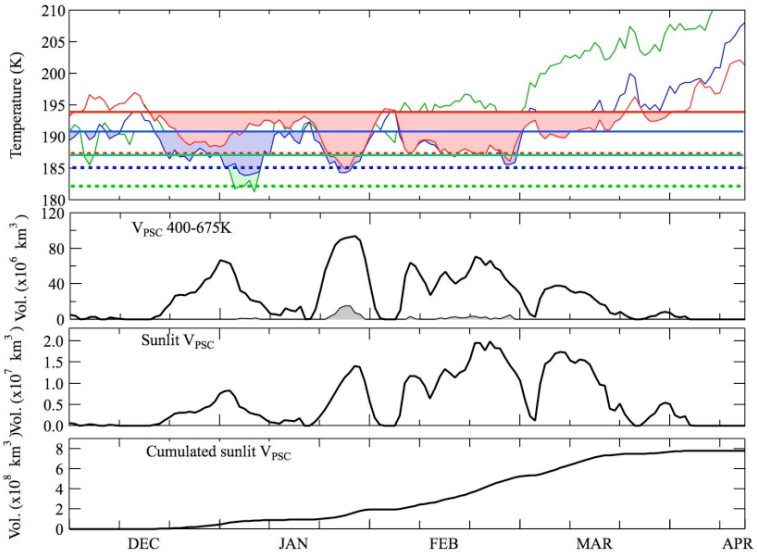

Fig. 5. Top: ECMWF ERA-Interim minimum temperature north of 60° N at 475 K (red), 550 K (blue) and 675 K (green) and NAT (solid lines) and ICE (dotted) threshold temperatures at the same levels. Bottom panels: PSC volume between 400–675 K, from top to bottom: (i) total volume below T_{NAT} (solid line) and T_{ICE} (grey area); (ii) sunlit (SZA < 93°) PSC volume indicative of chlorine activation; and (iii) integrated sunlit V_{PSC}.

ACPD
13, 311–343, 2013

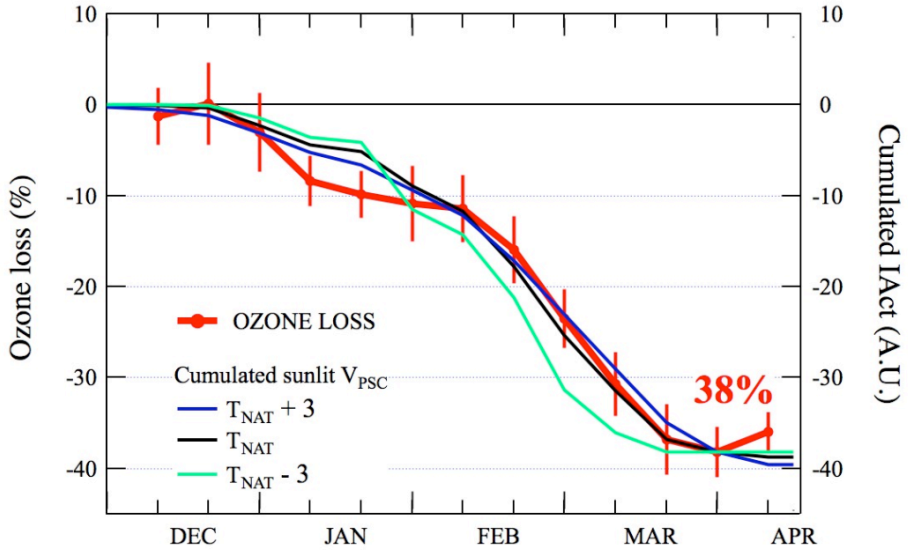

Fig. 6. O_3 loss and vortex sunlit weighted PSC cumulated volume calculated for $T_{NAT} - 3$ K (green), T_{NAT} (black) and $T_{NAT} + 3$ K (blue) normalised on 30 March.

ACPD
13, 311–343, 2013

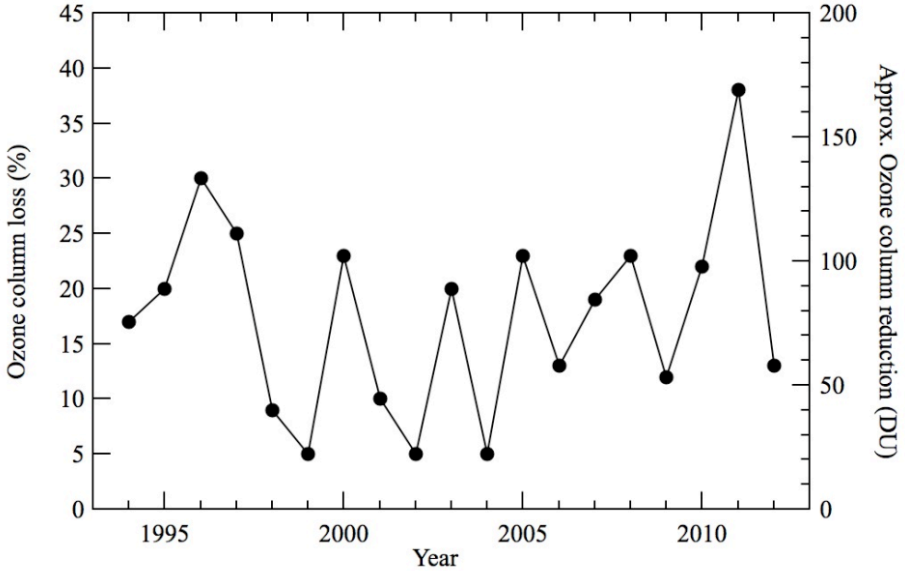

Fig. 7. Yearly ozone loss in the Arctic since 1994 derived from the measurements of the SAOZ/NDACC stations by the passive ozone method revisited using ERA-Interim reanalyses.

ACPD
13, 311–343, 2013

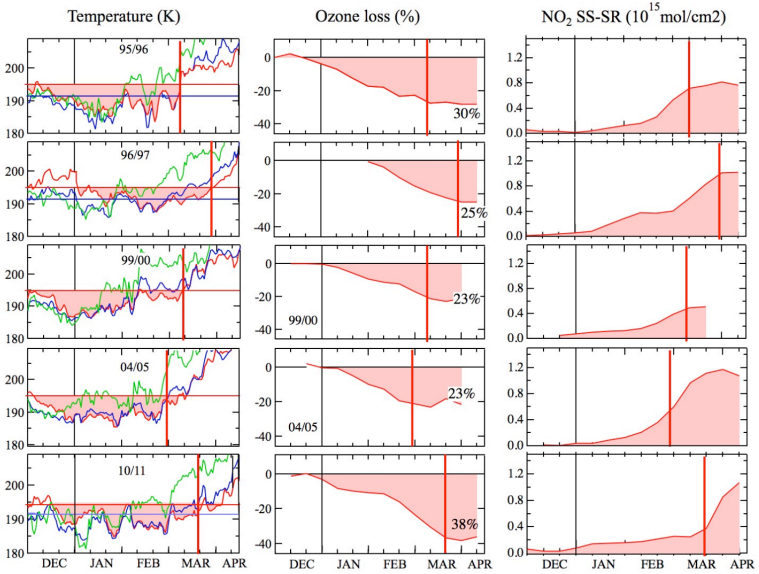

Fig. 8. Temperature, ozone loss and NO_2 diurnal variation during years of most important loss in the Arctic since 1994. Left: ERA-Interim minimum temperature north of 60° N at 475 K (red), 550 K (blue) and 675 K (green) and respective T_{NAT}; Middle: SAOZ ozone loss. Right: SAOZ NO_2 diurnal cycle amplitude. Shown by the vertical red bars are the dates of final warming. From top to bottom: 1995–96, 1996–97, 1999–00, 2004–05 and 2010–11.

ACPD
13, 311–343, 2013

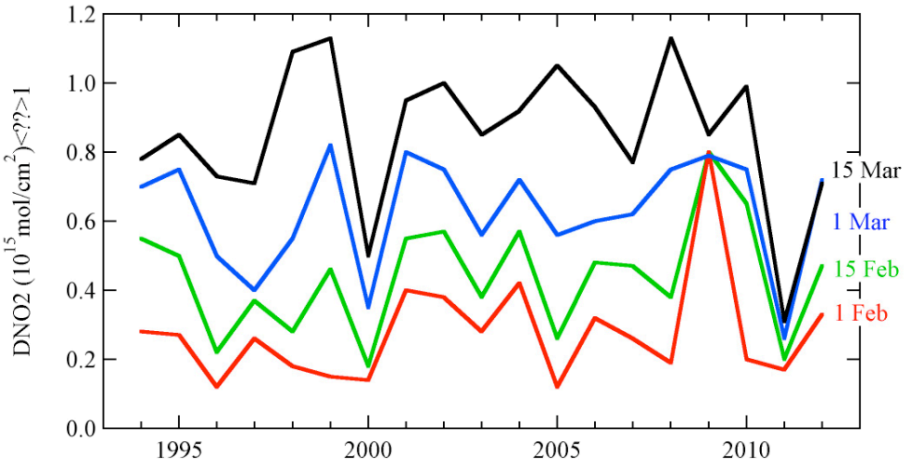

Fig. 9. NO_2 diurnal variation amplitude each year on 1 February, 15 February, 1 March and 15 March. Although large denoxification is frequent in early winter, it is generally followed by renoxification during the following weeks. 2011 is the only year of low NO_x until mid-March.

ACPD
13, 311–343, 2013

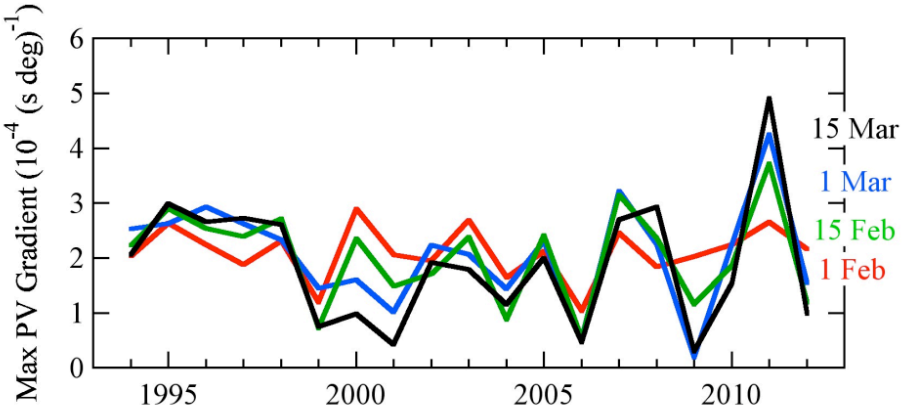

Fig. 10. Maximum PV gradient at 475 K indicative of vortex strength. The 2011 vortex was stronger than all others after mid-February.

ACPD
13, 311–343, 2013

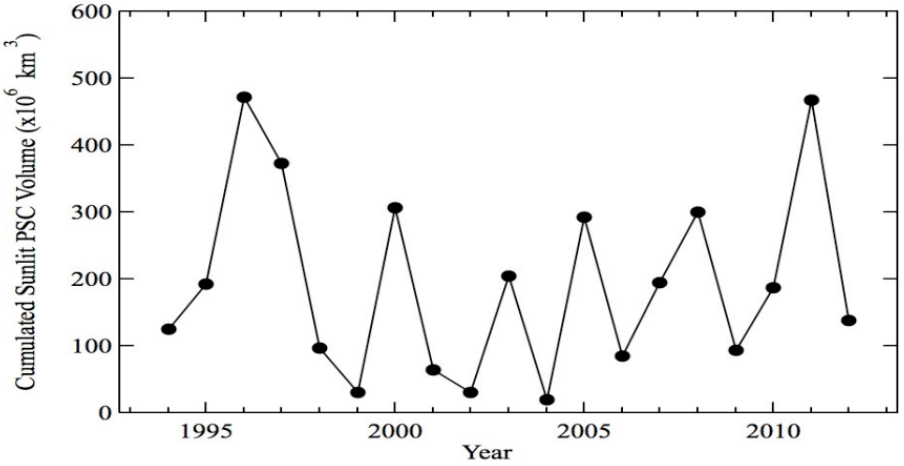

Fig. 11. Cumulated sunlight VPSC between 400–675 K since 1994. The PSC volume in 2011 was of same order of magnitude to that of 1996.

ACPD
13, 311–343, 2013

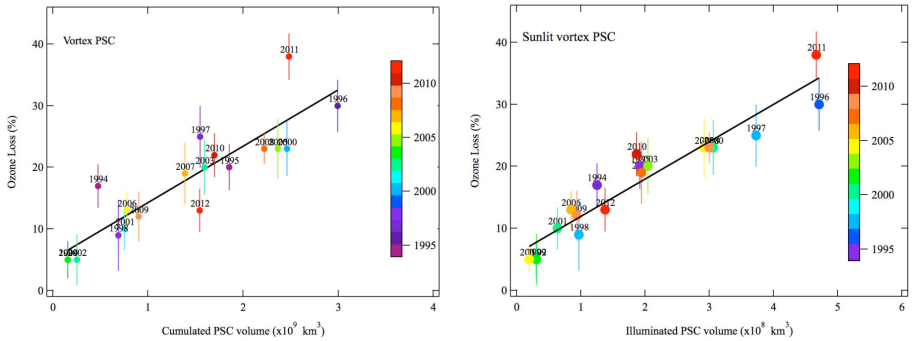

Fig. 12. Relationship between ozone loss and V_{PSC} between 400–675 K calculated from ERA-Interim temperatures. Left: V_{PSC} inside vortex; Right: sunlit V_{PSC} only, indicative of potential chorine activation. The selection of sunlit V_{PSC} instead of total V_{PSC} increases the correlation from 0.88 to 0.95. Although VPSC was similar or larger in 1996 than in 2011, the ozone loss was smaller, implying that another proxy, the state of denoxification, controls its amplitude.

ACPD
13, 311–343, 2013

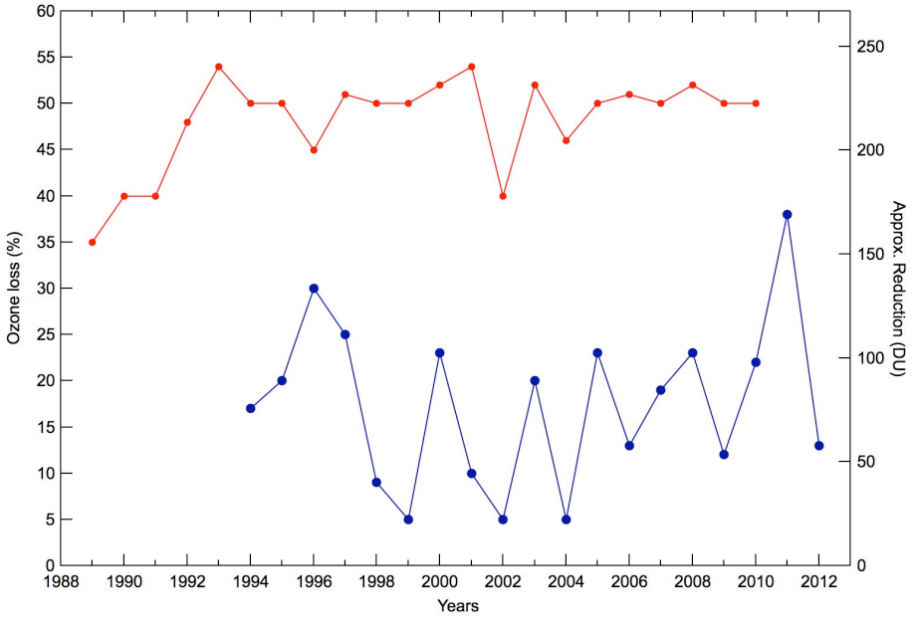

Fig. 13. Total ozone losses calculated between 1989–2012 from the SAOZ network and the passive ozone technique in the Arctic (blue) and the Antarctic (red). The amplitude of the 2011 Arctic depletion was similar to that of the 2002 Antarctic ozone hole.

ACPD
13, 311–343, 2013